Review Article

Chemical Review and Letters
journal homepage: www.chemrevlett.com
ISSN (online): 2645-4947 (print) 2676-7279

Alizarin Red S Dye Removal from Synthetic Effluent Solution Using Untreated Typha Grass Adsorbent

Abdullahi Muhammad Ayuba[a] and Musa Sani[a]*

[a]*Department of Pure and Industrial Chemistry, Faculty of Physical Sciences, Bayero University, Kano, Nigeria*

ARTICLE INFO

Article history:
Received 28 February 2023
Received in revised form 19 October 2023
Accepted 22 November 2023
Available online 26 October 2023

Keywords:
Adsorption
Alizarin Red S
Equilibrium
Kinetics
Thermodynamic
T. Latifolia

ABSTRACT

The adsorption of an anionic dye (ARS) on raw Typha grass (RAW-TG) was studied using an equilibrium batch approach. To test their impact on the ARS removal, the operational parameters of contact time (15 minutes), starting dye concentration (120 mg/L), adsorbent dosage (0.02 g), and pH (8) were tuned. Among the physical properties that were looked at were the RAW-TG's bulk density (0.397 g/cm^3), pore volume (1.253 cm^3), and moisture content (17.80 %). To better characterize the adsorbent, it was further studied using scanning electron microscope (SEM), Fourier transform infrared spectroscopy (FT-IR), and point of zero charges (PZC) techniques. To numerically model equilibrium data, the Langmuir, Freundlich, Temkin, and Dubining Radushkevich (D-R) models were utilized. Pseudo-first-order, pseudo-second-order, Elovich, and Intraparticle diffusion models were used to calculate the adsorption kinetics. Using the Van't Hoff plot, the thermodynamic parameters affecting the adsorption process were calculated. The data were presented most effectively by a pseudo-second-order model with a maximum adsorption capacity of 46.511 mg/g, and Freundlich's interpretation of the adsorption isotherm was significantly more favorable than that of the other models examined. According to the thermodynamic characteristics, the process was viable and spontaneous, with adsorption values of ΔG (-6.737 to -8.271 kJ/mol), ΔH (16.616 kJ/mol), and ΔS (16.616 J/molK, respectively. The findings of this investigation demonstrate that RAW-TG is an efficient, reasonably priced, and environmentally friendly adsorbent for the removal of ARS dye from aqueous solutions.

1.Introduction

Dye is one of the most significant and fundamental pollutants in wastewater. Due to the process of industrialization's increased mechanization, a substantial amount of wastewater containing colors is generated from numerous industrial and human activities [1]. The bulk of dyes discharged into the environment are synthetic dyes, which are non-biodegradable and contribute to environmental issues caused by dyestuff pollution. Therefore, before dye-containing wastewater is released into the environment, a treatment process should be carried out [2]. It is generally known that the adsorption approach for dye removal from effluents is affordable, secure, and simple to apply [3]. However, a variety of physicochemical processes, such as electrocoagulation, photocatalysis, flocculation, ozonation, adsorption, and membrane filtration, have been included in wastewater treatment systems [4].

This study examines the Typha grass (*T. latifolia*), which is commonly accessible and reasonably priced, for its ability to absorb the Alizarin red S dye from an aqueous

* Corresponding author.; e-mail: musaniyaya@gmail.com
https://doi.org/ 10.22034/CRL.2023.387634.1206

solution. Using the batch approach, it was determined how several parameters, such as contact time, adsorbent dose, initial concentration, pH, and temperature, affected the Alizarin red S dye's adsorption efficiency. Using the pseudo-first order, pseudo-second order, Elovich, and Intraparticle diffusion models, the kinetics of Alizarin red S dye adsorption onto untreated Typha grass was investigated. By fitting experimental equilibrium data to the Langmuir, Freundlich, Temkin, and Dubinin Radushkevich isotherm equations, the best-fit isotherm equation was found. The type of interaction between the ARS and RAW-TG surface will be evaluated using the thermodynamic data that was collected. The adsorption technique, specifically at low concentrations, is the most effective and economical way to treat wastewater containing dyes [5]. However, the adsorption capacity of the adsorbent under consideration determines how effective this strategy is [3].

2.Materials and Methods

2.1.Sample Collection and Preparations

The Typha grass was acquired in Jigawa State, Nigeria's Marma Town, Guri Local Government Area. The sample was washed twice to get rid of the impurities: once with tap water and once with distilled water [6]. The material was dried at 105 °C before being air dried. The dried material was ground into a powder, put through a 2 mm sieve, and given the designation RAW-TG. Alizarin Red S dye was purchased from Merck Chemicals. Ltd., Mumbai, India, whereas the reagents and chemicals utilized in this work were acquired from Sigma-Aldrich Ltd., London. These chemicals include hydrochloric acid (HCl), 36%, and sodium hydroxide (NaOH), 80%.

2.2. Preparation of Dye Solution

Distilled water was used to dissolve 1 g of Alizarin red S into 1 L, yielding 1000 mg/L as the stock solution. To create the experimental solutions at the necessary concentration, the stock solution was diluted with distilled water. It was purchased from Sigma Aldrich in the United Kingdom and has the following properties: molecular formula $C_{14}H_7NaO_7S$, molecular weight 342.253 g/mol, and is a poisonous, non-biodegradable, and water-soluble dye. Using a UV-Visible Spectrometer (Perkin Elmer, Lambda 35), the concentration of the unadsorbed ARS dye was determined at max = 424.89 nm.

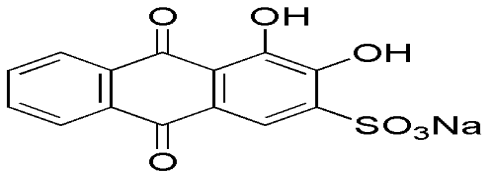

Fig 1: Chemical Structure of Alizarin Red S Dye

2.3 Characterization of the Adsorbent

By identifying the adsorbent's physical characteristics, such as bulk density, moisture content, and pore volume, the surface properties of the adsorbent were identified.

(a) Moisture Content Assessment

To do this task, the gravimetric method recommended by the AOAC [7] and others [8] was applied. 15 g of properly weighed RAW-TG were added to a weighted crucible. The crucible and its contents were initially dried in the oven for one hour at 130 °C. After cooling in a desiccator, it was reweighed. The weight was noted while the sample dried once more in the oven. After being heated for a second time for 30 minutes at 100 °C, the sample was cooled in a desiccator and weighed once again. The procedure was applied numerous times at the same temperature with breaks of 30 minutes to achieve a constant weight. Equation (1) was used to determine each sample's percentage moisture content:

$$\% \text{ moisture content} = \frac{W_2 - W_3}{W_2 - W_1} \times 100 \qquad (1)$$

Where W_1 is the crucible's weight, W_2 is the crucible's initial weight with the sample, and W_3 is the crucible's final weight with the sample.

(b) Determination of Bulk Density

The bulk density of RAW-TG was estimated using Archimedes' method by weighing a 10 cm^3 measuring cylinder before and after it was filled with samples, leveling it, and then weighing it again. The weight of the sample that was placed within was determined by comparing the weights of the filled and empty measuring cylinders. The amount of water in each measuring cylinder was calculated by multiplying the weight of the full and empty cylinders by two. Equation (2) [9] was used to get the bulk density:

$$\text{Bulk density} = \frac{W_2 - W_1}{V} \qquad (2)$$

(c) Determination of Pore (Void) Volume

To calculate the RAW-TG's pore volume, 2.0 g of the sample was cooked in water for 15 minutes. After the air in the pores had been expelled, the sample was gently dried and reweighed. The increase in weight was divided by the density of water to determine the pore volume. [8-9].

$$\text{Pore (Void) Volume} = \frac{W_2 - W_1}{\rho} \quad (3)$$

W_1= the beaker's starting weight with the sample (g), W_2= the beaker's final weight with the sample (g), and = the water's density (gcm^{-3}).

(d) Scanning Electron Microscopy (SEM)

The surface morphological change of the adsorbent sample was examined using a scanning electron microscope (Phenom-World Eindhoven). Adsorbent micrographs were scanned at a magnification of 500x and an accelerating voltage of 15 kV before and after ARS adsorption.

(e) Fourier Transform Infrared Spectroscopy (FT-IR)

Using an Agilent Technology Cary 630 spectrophotometer, a Fourier Transform Infrared (FT-IR) study of the adsorbent before and after ARS adsorption was performed. To conduct the analysis, the sample was scanned 32 times at a resolution of 8 cm^{-1} throughout a wave number range of 650 to 4000 cm^{-1}.

(f) Determining of Point of Zero Charge

Points of zero charges (PZCs) are pH values where, at a particular temperature, applied pressure, and aqueous solution composition, the surface charge components become equal to 0 [7]. The PZC provides useful information on the mechanisms of metal sorption. There are primarily three techniques for identifying the point of zero charges: the salt addition method, the zeta potential approach, and the ion adsorption technique. In this paper, the salt addition approach was used. Adsorbent PZC values were calculated in a 0.1 M $NaNO_3$ solution between 303 and 333 K. 40.0 mL of 0.1 M $NaNO_3$ solution received 0.2 g of the adsorbent sample. A pH meter (MP 220) was then used to modify the suspension's pH using 0.1 M HCl and 0.1 M NaOH to produce initial pH values of 2, 4, 6, 7, 8, and 12. After that, each flask was forcefully shaken for 24 hours in a shaker bath. The final pH of each sample was carefully assessed following settling. The final pH values were then plotted against the initial pH values (the difference between the final and initial pH) [8]. The PZC was defined as the initial pH value at which pH is zero [9].

2.4 Batch Adsorption Experiment

Batch studies were carried out to ascertain the optimal circumstances for the equilibrium adsorption of ARS onto raw Typha grass. The results of the optimization analysis were used to guide the batch adsorption studies. In a 250 cm3 conical flask, each of these systems was independently operated at 30, 40, and 50 ^{0}C. The conical flasks were covered during the equilibration period. They were then placed for the length of the optimization process on an Innova 4000 incubator shaker with temperature control. A Perkin-Elmer UV-visible spectrophotometer was used to analyze the filtrate at a maximum absorbance wavelength of 424.89 nm after the material had reached adsorption equilibrium. The extent of adsorption was calculated using equations (4) and (5) respectively.

$$\text{Adsorption Capacity } (q_e) = \frac{(Co - Ce)\,x\,V}{m} \quad (4)$$

$$\% \text{ adsorption} = \left(\frac{Co - Ce}{Co}\right) \times 100 \quad (5)$$

Where V is the volume of Alizarin red S solution (L), q_e is the adsorption capacity (mg/g), Co and Ce are the starting and final equilibrium concentrations (mg/L) of Alizarin red S in solution, m is the mass (g) of the adsorbent, and so on [5, 10].

3.Results and Discussion

3.1.Adsorbent Characterization

Table 1 shows the influence of certain significant physical characteristics of the adsorbent. The raw Typha grass adsorbents' bulk density, moisture content, and pore volume value all point to their having good adsorptive characteristics. Given that low moisture content and high pore volume have been found to significantly increase adsorption for both organic and inorganic species, respectively [11].

Table 1. Physical Properties of RAW-TG

Moisture Content (%)	Bulk Density (gcm^{-3})	Pore Volume (cm^3g^{-1})
17.80	0.397	1.253

Fig 2 shows the FT-IR spectra of the adsorbent before and after ARS adsorption. Fig 2 displays the FT-IR spectrum of RAW-TG with loaded ARS equivalents. Before adsorption, RAW-TG showed peaks at 3327, 2918, 1607, 1514, and 1104 cm^{-1}, which were attributed to, respectively, O-H stretching, C-H stretching, C=O stretching, and C=C stretching (Table 2) [11, 12]. Before adsorption, the free O-H stretch for RAW-TG emerged at 3327 cm^{-1}. There was a change in the free O-H stretch's vibration frequency following the loading of RAW-TG

with ARS. The binding of ARS to the surface of the adsorbents may be the cause of these changes in vibration frequency [13]. However, some changed peak positions and the emergence of some new peaks in the FT-IR spectrum following adsorption also point to interactions between the adsorbents and adsorbates. Additionally, the carboxylic acids group found in the adsorbents is responsible for the existence of the hydroxyl and carbonyl groups. Important adsorption sites include hydroxyl, carboxyl, and carboxylic acids [14].

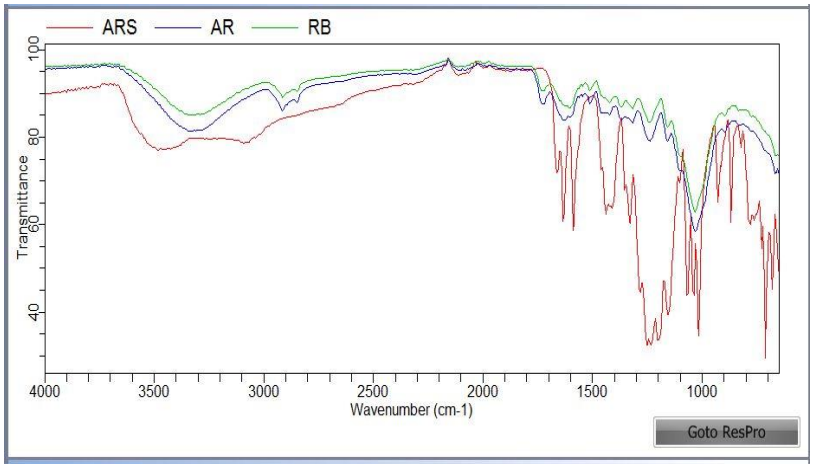

ARS= ALIZARIN RED S, AR= RAW ADSORBENT AFTER ADSORPTION, RB= RAW ADSORBENT BEFORE ADSORPTION

Fig 2. Overlaid FT-IR spectrum ARS and RAW before and after adsorption (ARS = Alizarin Red S, RAW-TG after adsorption onto Alizarin Red S, RAW-TG before adsorption)

Table 2: Different functional groups recognized before and after adsorption of ARS onto RAW-TG

Functional Group	Adsorption range (cm^{-1})	Before adsorption (cm^{-1})	After adsorption onto ARS (cm^{-1})	Difference (cm^{-1})
OH stretch	3700-2500	3327	3335	13
C-H stretch	3000-2840	2918	2918	0
C=O stretch	1710-1580	1607	1629	12
C≡C stretch	1675-1550	1514	1514	0
C-O stretch	1080-1300	1104	1104	0

Fig 3 shows SEM images of the adsorbents both before and after ARS was adsorbed to them. However, the machine was run at a 15.00 kV accelerating voltage and 300–1000x magnification. Before adsorption, RAW-TG micrographs show a surface that is somewhat rough and has flaws and dumps. This surface roughness could be caused by adhering particles, which could be dust or other contaminants [15].

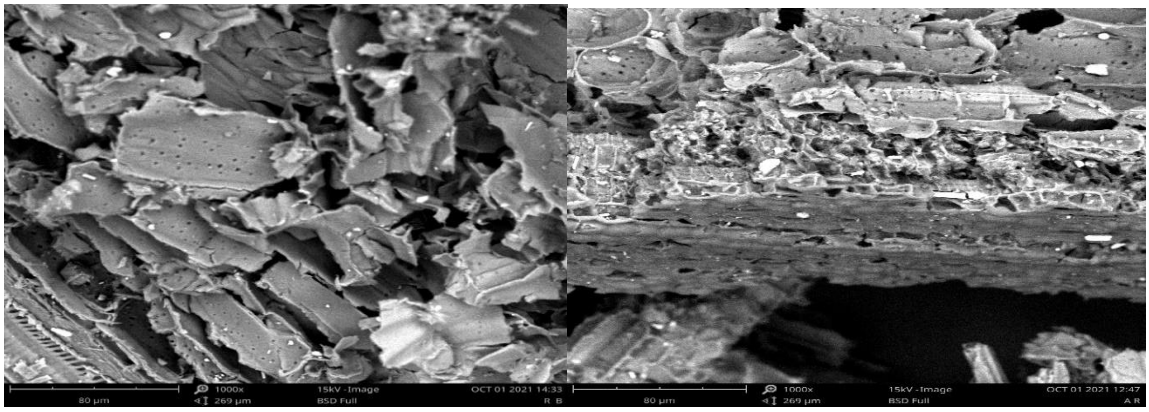

(a) (b)

Fig 3. SEM Micrograph of RAW-TG (a) before and (b) after adsorption of ARS

3.3 Determination of Point of Zero Charge

The points of zero charge (PZCs) result for RAW-TG adsorbent is shown in Fig 4. The PZC studied is 6.03, which indicates the presence of perfect charge balance in the acidic medium the region among the equilibrated ions in an aqueous solution. Furthermore, substrates with low PZC values have a strong tendency to treat cation-contaminated effluents, whereas substrates with high PZC values would be better suited to collect [16].

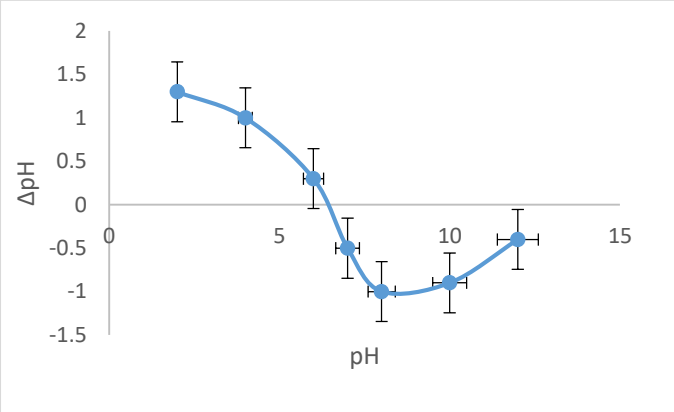

Fig 4. Point of zero charges (PZC) of RAW-TG

3.4.Batch Adsorption

(a) Effect of Contact Time

The contact time effect, which is depicted in Fig 5, is one of the major variables affecting the efficacy of the adsorption. In this experiment, 20 cm^3 of a 50 mg/L ARS solution and 0.02 g of RAW-TG, respectively, were added. The efficacy of the adsorption was then increased by rotating the vortex at varying intervals. The adsorption equilibrium has been reached and the clearance rate is greater than 70 % after 15 minutes in the vortex. However, the rate of adsorbate removal began rapidly before gradually reducing until it achieved equilibrium. This may be because there are initially a large number of open surface sites accessible for adsorption, but as time passes, the solute molecules in the solid and bulk phases develop repellent forces that make it challenging for the open surface sites to be filled. Other authors [17] reported similar results.

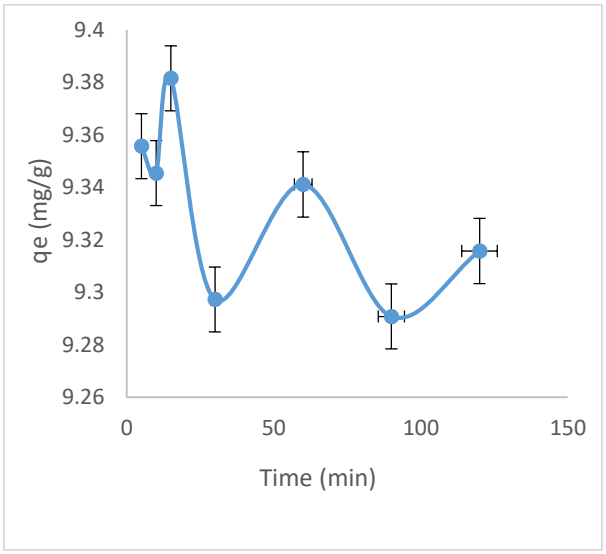

Fig 5. Effect of contact time on the adsorption of ARS onto RAW-TG

(b) Effect of Adsorbent Dosage

Fig 6 depicts the profile diagram of the RAW-TG doses thought to be effective in removing adsorbates. Adsorbent dosages ranging from 0.02 g to 0.2 g were added to the ARS solution at an initial concentration of 50 mg/L. With an increase in adsorbent dosage, the removal efficiency of ARS was quickly reduced until the ideal was reached. For this experiment, 0.02 g was the ideal dosage, and the adsorption capacity was 49.92 mg/g. [18].

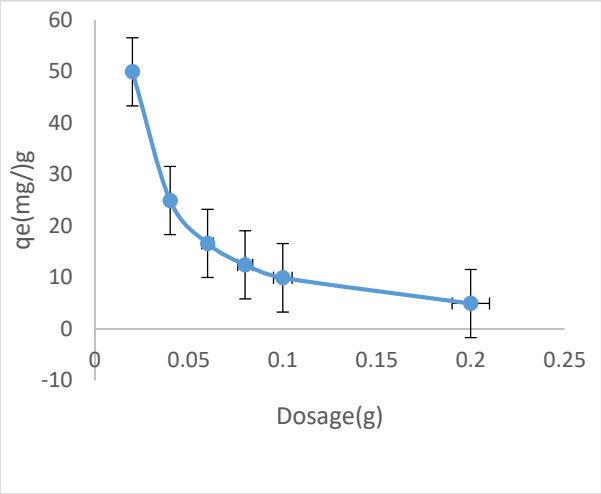

Fig 6. Effect of Adsorbent Dosage on the Adsorption of ARS onto RAW-TG

(c) Effect of Initial Concentration

The adsorption of ARS onto RAW-TG was affected by the initial dye concentration (50 mg/L), as shown by the curve in Fig 7. It was found that the total amount of ARS absorbed per gram of the adsorbent rose as concentration increased. As ARS dye in the aqueous phase interacts more strongly with the active sites of the adsorbent at high concentrations than it does at low concentrations, the driving force required to transfer ARS onto RAW-TG particles also increases at higher concentrations [19].

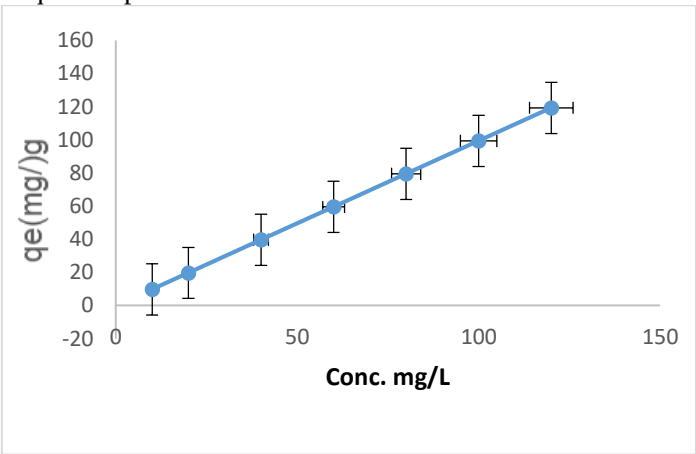

Fig 7. Effect of Initial Concentration on the Adsorption of ARS onto RAW-TG

(d) Effect of pH

Fig 8 illustrates how pH affects the adsorption of ARS onto untreated Typha grass. The adsorbent's capacity for absorption increased up to pH 8, and basic pH, which elevated pH from 2 to 10, significantly impacted ARS approval. While the initial concentration and pH were 50 mg/L and 7, respectively, the maximum quantity of ARS dye was absorbed by untreated typha grass at pH 8, resulting in a 47.99 mg/g adsorption capacity. The existence of essential functional groups on the surface of RAW-TG may be the reason for this outcome [19]. The lowest absorption capacity, however, was found to be at pH 4, while its highest was found to be at pH 8 [20].

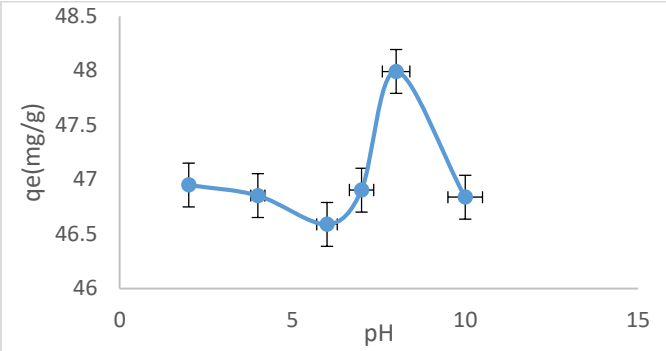

Fig 8. Effect of pH on the Adsorption of ARS onto RAW-TG

3.5 Adsorption Kinetics

Data on absorption rate, which is essential for creating and modeling the adsorption processes, is provided by the kinetic studies, which are significant [22]. Therefore, to comprehend the adsorption mechanism, the removal rate and equilibrium time are still crucial [17]. The data from batch adsorption investigations, in which samples were withdrawn at intervals of 10 for a maximum of 120 minutes, were subjected to several kinetic models. This may make it possible to ascertain how the dye interacts with the surface of the adsorbent (RAW-TG). These models were evaluated, reported on, and discussed.

(a) The pseudo-first-order

The pseudo-first-order equation is generally expressed as follows [23]:

$$\frac{dq_t}{dt} = k_1(q_e - q_t) \qquad (6)$$

Where: q_e and q_t are the adsorption capacity at equilibrium and at time t, respectively (mg/g), k_1 is the rate constant of pseudo-first-order adsorption (L/min). After integration and applying boundary conditions t = 0 to t = t and q_t = 0 to q_t = q_t, the integrated form of Eq. (6) becomes:

$$\log(q_e - q_t) = \log(q_e) - \frac{k_1}{2.303}t \qquad (7)$$

The values of log (q_e - q_t) were linearly correlated with t. The plot of log (q_e - q_t) vs. t should give a linear relationship from which k_1 and q_e can be determined from the slope and intercept of the plot respectively (Fig. 9a).

(b) The pseudo-second-order equation

The kinetic rate equation for the pseudo-second-order adsorption is expressed as:

$$\frac{dq_t}{dt} = k_2(q_e - q_t)^2 \qquad (8)$$

The pseudo-second-order adsorption rate constant is K_2 (g.mg^{-1}min^{-1}). For the boundary conditions t = 0 to t = t and q_t = 0 to q_t = q_t, the integrated form of Eq. (8) becomes:

$$\frac{1}{(q_e - q_t)} = \frac{1}{q_e} + K_t \qquad (9)$$

Equation (6) was rearranged to obtain Eq. (9), a linear form:

$$\frac{t}{q_t} = \frac{1}{K_2 q_e^2} + \frac{1}{q_e}(t) \qquad (10)$$

The initial adsorption rate, h (mg.g^{-1}min^{-1}) is;

$$h = K_2 q_e^2 \qquad (11)$$

Then equation (8) becomes

$$\left(\frac{t}{q_t}\right) = \frac{1}{h} + \frac{1}{q_e}(t) \qquad (12)$$

The plot of (t/q_t) against t of Eq. (12) gives a linear relationship from which K_2 and q_e can be obtained from the intercept and slope of the plot respectively (Fig. 9b).

c) Elovich Equation

The Elovich kinetic model is defined by the following relation [24].

$$q_t = {}^1/_{\beta}\ln(\alpha\beta) + \left({}^1/_{\beta}\right) lnt \qquad (13)$$

The magnitude of the surface activity and activation energy for the adsorption process are both usefully described by this model. The parameters *(α)* and *(β)* were calculated from the slope and intercept of the linear plot of *q*t versus ln (t) (Fig. 9c).

(d) Intraparticle Diffusion Equation

An empirical model called the Dubinin-Radushkevich isotherm was first developed to explain how subcritical vapors may adhere to micropore solids by a pore-filling mechanism [31]. The linear version of the Dubinin-Radushkevich (D-R) isotherm model is given by equation (19).

$$lnqe = lnqm - \beta\varepsilon^2 \qquad (19)$$

$$\varepsilon = RTln\,[1 + 1/Ce] \qquad (20)$$

$$E = 1/\sqrt{2\beta} \qquad (21)$$

The D-R correlation coefficient is the lowest (R2) in comparison to all the studied isotherms, so the D-R model exhibited less fit with the experimental data. The E value

was less than 8 kJ mol-1 implying that the adsorption process is governed by physical forces [33]. The Dubinin-Rudushkevich (D-R) model mean free energy (E) yields data on the chemical or physical characteristics of the adsorption process.

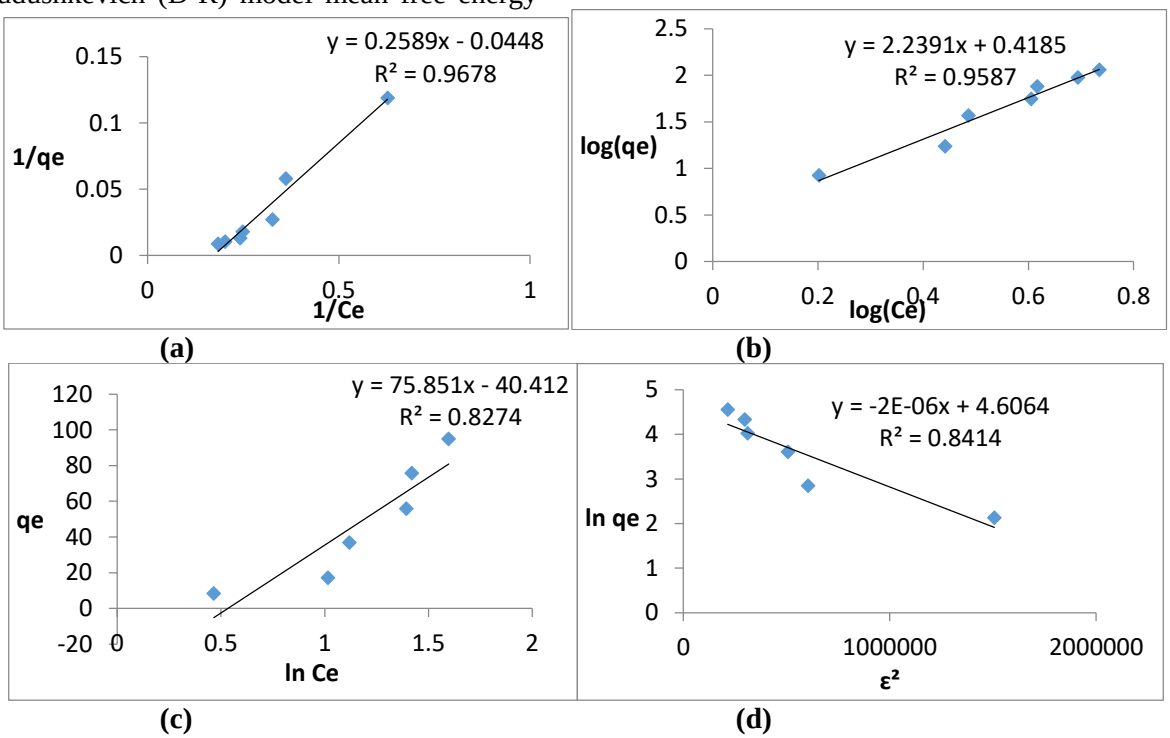

Fig 9. Adsorption isotherms plots for (a) Langmuir (b) Freundlich (c) Temkin (d) Dubinin-Radush-kevich for the adsorption of ARS onto RAW-TG

Table 4. Adsorption Isotherm constants for the adsorption of ARS onto RAW-TG

Parameter	**Alizarin Red S**
Langmuir	
Q_O(mg/g)	-9.3720
K_L(L/mg)	-0.1660
R_L	-0.1115
R^2	0.967
Freundlich	
1/n	1.0029
N	0.4992
K_F	1.2083
R^2	0.958
Temkin	
A_T	0.5288
B_T	86.09
B	29.259
R^2	0.827
Dubinin-Radushkevich	
q_m(mg/g)	48.638
K_{dr}(mol^2/KJ^2)	3.0×10^{-6}
E(KJ/mol)	4.0×10^{-1}
R^2	0.841

3.7 Thermodynamic Studies

Changing the temperature from 30 °C to 50 °C (303-323 K) while keeping optimal values for all other variables, such as contact time, pH, adsorbent dosage, agitation speed, and initial ARS concentrations, allowed researchers to study the impact of temperature on the adsorption of Alizarin Red S onto RAW-TG.

Using thermodynamic metrics such as changes in free energy (ΔG), enthalpy (ΔH), and entropy (ΔS), which are calculated using equations (22), (23) and (24), it is possible to immediately assess the viability and spontaneity of the adsorption process:

$$\Delta G = -RT\ln K_L \quad (22)$$

$$\Delta G = \Delta H - T\Delta S \quad (23)$$

Where R is the gas constant (8.314 J/molK), T is the absolute temperature (K), and K_L is the thermodynamic equilibrium constant,

From equations (22) and (23) we get equation (24)

$$\ln K_L = -\frac{\Delta H}{RT} + \frac{\Delta S}{R} \quad (24)$$

The plot of $\ln K_L$ (L/mol) versus 1/T (Van't Hoff) was constructed and ΔH and ΔS values were calculated from the slope and intercept of the plot, and K_L is equal to qe/Ce obtained at different temperatures [34].

Table 5. Thermodynamic parameters for the adsorption of Alizarin red S onto RAW-TG

T (K)	K_L	ΔG (kJ/mol)	ΔH (kJ/mol)	ΔS (J/mol.K)
303	14.503	-6.737	16.616	77.424
313	20.399	-7.847		
323	21.757	-8.271		

The ARS elimination process is spontaneous and acceptable from a thermodynamic perspective, as shown by the negative Gibbs free energy (ΔG) in Table 5. Higher temperatures increase the negative value, indicating that RAW-TG is more effective in absorbing the adsorbate at higher temperatures within the measured range [34]. The positive value of the enthalpy change (ΔH) indicates that the adsorption process is endothermic. The magnitude of the enthalpy shift (ΔH) can provide insight into the nature of the active adsorption process. If the value of ΔH is greater than 80 kJ/mol, the process is known as chemisorption, which involves chemical bonding between the adsorbate and adsorbent surface. However, if ΔH is less than 80 kJ/mol, it means that the system under study is one in which physisorption is the adsorption mechanism [35, 36].

Conclusion

According to the study's findings, Typha grass that hasn't been treated works well as an adsorbent to take out anionic dye (ARS) from aqueous solutions. For the adsorbent, the effects of contact time, adsorbent dose, starting ARS concentration, pH, and temperature were investigated because they all have a major impact on adsorption efficiency. The Freundlich isotherm model offered the most accurate explanation of the adsorption isotherms, and the pseudo-second-order model successfully justified the observed adsorption kinetics. The computed thermodynamic properties, such as enthalpy, entropy, and Gibb's free energy, were used to determine whether the adsorption process was spontaneous and practicable. The findings indicated that RAW-TG might work well as an adsorbent to remove wastewater-borne anionic dyes like Alizarin Red S.

Acknowledgment

For their cooperation with the characterization of the adsorbent, the authors are grateful to Musa Garba Beli, Mr. Muhammad Buhari Umar, and Mal. Usman Muhammad of Bayero University's Chemistry Department in Kano.

References

[1] A. J. Jafari, B. Kakavandi, R. R. Kalantary, H. Gharibi, A. Asadi, A. Azari, A. A. Babaei, A. Takdastan, *Korean J. Chem. Eng*. 33(10) (2016) 2878–2890.

[2] J. N. Putro, J. Yi-Hsu, F. E. S. Ju, S. P. Santoso, S. Ismadji, *Green Chem. and Wat. Remed.* 5 (3) (2021) 67-84 https://doi.org/10.1016/B978-0-12-817742-6.00004-9.

[3] A. M. Ayuba, B. Idoko, *Arab. J. of Chem. and Env. Res.*, 08(01) (2021) 114–132

[4] H. Wang, X. Lai, W. Zhao, Y. Chen, X. Yang, X. Meng, Y. Li, *R. Soc. of Chem. J*. 9 (2019) 21996–22003.

[5] M. Siminghad, S. Sheshmani, A.S. Shahvelayati, (2021) *Int. J. Environ Anal. Chem.* 101(4), pp.473-481.

[6] F. O. Nwosu, F. A. Adekola, A. O. Salami, *Pak. J. Anal. Environ. Chem.* 18 (1) (2017) 69. https://doi.org/10.21743/pjaec/2017.06.07.

[7] AOAC *Official Methods of Analysis.* AOAC International Washington D.C 17th Edn. 1456-1500 (2005).

[8] A. M. Ayuba, B. Idoko, *Appl. J. of Envir. Eng. Sci.,* 6(2) (2020) 182-195.

[9] E. N. Bakatula, D. Richard, D. Neculita, C. M. Zagury, J. Gerald, *Envir. Sci. and Poll. Res.* (2008).

[10] E. Sebata, M. Moyo, U. Guyo, N. P. Ngano, B. C. Nyamunda, F. Chigondo, M. S. Chitsa, *Intl. J. Eng. Resear. & Tech.* 2 (5): 312 – 321 (2013).

[11] A. A. Werkneh, N. G. Habtu, H. D. Beyene, *Amer. J. of Appl. Chem.* 2(6) (2014) 128-135.
[12] J. O. Babalola, J. O. Olowoyo, A. O. Durojaiye, A. M. Olatunde, E. I. Unuabonah, M. O. Omorogie, *J. Tai. Inst Chem. Eng.* 58 (2016) 490–499
[13] U. Itodo, A. Usman, C. Ugboaja, *J. Encap. and Adsorp. Sci.*, 1 (2011) 57- 64.
[14] S. Chowdhury, R. Mishra, P. Saha, P. Kushwaha, *Desal.* 265 (2011) 159–168 doi:10.1016/j.desal.2010.07.047.
[15] A. Mukherjee, A. R. Zimmerman, W. Harris, *Geoderma* 163(3-4) (2011) 247–255. https://doi.org/10.1016/j.geoderma.2011.04.021
[16] N. Abdus-Salam, S. K. Adekola, *App. Water Sci.*, (2018) 28-222. https://doi.org/10.1007/s13201-018-0867-7.[17] C. Li, N. C. Zhang, J. Jixiao, X. Jiawen, W. Liu, Z. Jianli, Y. Ma, *J Env. Poll.* 255 (2019) 113150 https://doi.org/10.1016/j.envpol.2019.113150.
[17] G. Sposito, The chemistry of soils, 2nd. Oxford University Press, New York (2008).
[18] Q. Liu, B. Yang, L. Zhang, R. Huang, *Int. J. of Biol. Macromo.* 72 (2015) 1129–1135.
[19] N. Yeddou, A. J. Bensmaili, *Chem. Soc. Niger*, 36(2) (2007) 52–58.
[20] F. O. Nwosu, F. A. Adekola, A. O. Salami, *Pak. J. Anal. Environ. Chem.* 18 (1) (2017) 69. https://doi.org/10.21743/pjaec/2017.06.07.
[21] C. Aharoni, M. Ungarish, *J. Chem. Soc., Trans. 1: Physical Chemistry in Condensed Phases*, 73 (1977) 456-464.
[22] A. M. Ayuba, M. Ladan, A. S. Muhammad, *Appl. J. Environ. Eng. Sci*. 6(3) (2020) 213-226.
[23] S. Guo, X. Liang, N. Feng, Q. Tian, *J. Hazard. Mater*. 174 (2010) 756–762.
[24] W. J. Weber, J. C. Morris, *J. Appl Sci. Eng.* 89 (2) (1963) 31-60.
[25] T. H. Vermeulan, K. R. Vermeulan, L. C. Hall, *Ind. Eng. Chem*. (1966) 212-223.
[26] I. Langmuir, *J. Am. Chem. Soc*. 40 (1918) 1362-1403.
[27] G. Mckay, H. S. Blair, J. R. Gardiner, *J. Appl. Polym. Sci.*, 29(5) (1984) 1499-1514.
[28] S. Alibakhshi, A.S Shahvelayati, S. Sheshmani, M. Ranjbar, S. Souzangarzadeh, (2022). *Nature*12 (1), p.12431.
[29] N. D. Hutson, R. T. Yang, *Alch. Journal* 46 (11) (2000) 2305-2317.
[30] M. I. Temkin, V. Pyzhev, *Acta. Phys. Chim. Sin., USSR*. 12 (1940) 327-356.
[31] T. Smith, T. Santhi, A. L. Prasad, S. Manonmani, *Arab. J. Chem*. 10 (2017) S244–S251.
[32] M. M. Dubinin, L. V. Radushkevich, *P. Natl. Acad. Sci. USA.* 55 (1947) 331-337.
[33] E. R. Ushakumary, G. Madhu, *Int. J. Environ.Waste Manag.* 13(1) (2014) 75-89.
[34] M. Sabbaghan, A.S. Shahvelayati, (2016). *Ceram. Int.*, 42(3), pp.3820-3825
[35] K. Sumanjit, T. P. S. Walia, *J. Environ. Eng. Sci*.7 (5) (2008) 433-438.
[36] E. Akar, A. Altinisik, Y. Seki, *J. Eco. Eng.* 52 (2013) 19–27.